The International Journal of Advanced Manufacturing Technology (2019) 100:2803–2811
https://doi.org/10.1007/s00170-018-2834-8

ORIGINAL ARTICLE

Completely in situ and non-contact warpage assessment using 3D DIC with virtual patterning method

Jae B. Kwak[1]

Received: 3 July 2018 / Accepted: 2 October 2018 / Published online: 22 October 2018

Abstract
Recently, advanced experimental mechanics have been developed using optical techniques for measuring 3D deformations of objects in industries. Especially, Moiré systems and 3D DIC (digital image correlation) were competing in characterizing warpage behaviors of electronics package under thermal loading with consideration of manufacturing process, which is accompanied by elevated temperatures. Both techniques conventionally require various surface treatments either physically or chemically, which involves contaminations on measuring objects. Additionally, excessive surface treatment results in reduction of measurement accuracy. Thus, in this study, truly in situ and non-contact 3D DIC method is developed using virtually generated speckle pattern. A commercial DLP (digital light processing) projector together with devised collimate lens system is used to project proper image of speckles on surface of specimen. The collimate lens system fully controls size of speckle image on such small area of electronics package. The feasibility of 3D DIC with virtual pattern is validated, and warpage characterization of PBGA (plastic ball grid array) package (15 mm × 15 mm) is successfully demonstrated.

Keywords DIC (digital image correlation) · DLP (digital light processing) · PBGA (plastic ball grid array) · Electronics package · Warpage

1 Introduction

Due to an increasing demand for miniaturization of electronic devices while number of input/output of electrical signals increases, there are increasing needs for experimental methods that can be used to quantify the shape and deformations at reduced scales. Particularly, warpage measurement is one of the most common interests due to composite nature of electronic packages subjected to various temperature levels during manufacturing or service [1, 2]. Since DIC is advantageous in terms of its non-contact full-field measurement nature and robustness in correlation algorithm, DIC technique has been widely adopted in industries. DIC is based on tracking speckle patterns before and after deformation to determine the full-field surface displacement and strain for general material system. Especially, 3D DIC technique consists of two CCD (charge coupled device) cameras and exhibits unique benefit of providing in-plane and out-of-plane deformations and strain tensors at the same time. This enables 3D DIC to cope the shortfalls of other optical measurement methods such as Moiré systems [3].

The two key parameters in DIC technique are speckle pattern on sample surface and lighting. Appropriate speckle size of pattern is generally determined based on FOV (field of view) size, while the measurement sensitivity is determined by the uniformity of light distribution. If these conditions are well satisfied, then its empirically determined sensitivity is known to be 1/50000 of FOV size in length. However, it is quite challenging to obtain proper speckle size with sprayed pattern and uniform light distribution, especially for small-scale measurements and for objects of complex geometries. Normally, ceramic sprays are used for thermal deformation measurements, assuming spray particle itself would never be deformed during experiments. However, the particle size of these ceramic or enamel spray is usually 50~100 um, which may mislead the DIC results in the measurements dealing with few hundreds microns deformations. Also, it cannot be applied to measure such thin objects.

Previously, many researchers investigated and developed advanced experimental mechanics using DIC technique, such as

✉ Jae B. Kwak
jaekwak@chosun.ac.kr

[1] School of Mechanical System & Automotive Engineering, Chosun University, 309 Pilmun-daero, Dong-gu, Gwangju 61452, South Korea

materials characterization with microscopic 2D DIC [4–8], dynamics of vibrational movement with high-speed 3D DIC [9], and crack or stress analysis under bending or tensile test with 3D DIC [10, 11]. In addition, Guangyao Li et al. and Jianwei Liu et al. applied 3D DIC to analyze the mechanical property of the weld line and flow stress of the thin-walled tube during hydroforming process respectively [12, 13]. Most of these DIC experiments are various pattern generation techniques that are spraying paint with atomizer, drawing with pen, and using its original surface textures after etching process [14]. Even Wang et al. developed their own pattern generation method using spin coating with powder and resin [15]. In addition, Chen et al. devised a method to transfer patterns on the surfaces [16]. Yet, these are still involving chemical or physical surface treatment.

Mostly, it is not desirable or not allowed to contaminate the specimen with speckle process when 3D DIC is adopted in manufacturing site. In this regard, a pattern projection (virtual patterning) as an alternative way of speckle generation can be considered. Therefore, this study introduces the pattern projection method using the commercial DLP projector with devised lens system consisting of two different lenses for adjusting size of the pattern image. A DLP projector is a type of projector based on the digital light processing chip. The color passes via the chips, then feeds the image through the projection optical system, and then appears onto the projection screen with a magnified image size. The devised collimate lens system allows an image of pattern to be focused on the specimen surface with properly sized speckles. Then, this pattern projection method is applied to 3D DIC for surface profiling, and the measurement result is compared with other optical profilometer in order to validate the measurement accuracy and sensitivity level.

For electronics package assembly, reflow process is known to be the most economic and efficient as surface mount technology. Reflow process uses convection chamber to melt fine solders and induces metallurgical bonding between the electronics package and PCB (printed circuit board). During reflow process, electronics packages are subjected to undergo high temperatures and resulted in warpage (out of plane deformation) due to the nature of composite. Warpage behavior significantly affects manufacturability and long-term reliability [17–19]. In this regard, as one of PBGA (plastic ball grid array) package, a memory unit of POP (package on package) was selected in this study [20, 21]. The newly developed pattern-free 3D DIC is introduced to apply for truly in situ and non-contact warpage measurement.

2 Schematic of 3D DIC for shape profile measurement

The object under test is viewed by a stereo CCD cameras for measuring the 3D displacements (see Fig. 1a). 3D DIC is a consequent combination of two cameras' image correlation and photogrammetry resulting in 2D and 3D deformation, 3D shape profile, and plane strain tensor under various loading conditions. In DIC measurements, conventionally, a random pattern with contrast is applied to the surface of the test object (see Fig. 1b), which deforms along with the object. Then, images of the objects while deforming are sequentially recorded by the CCD cameras and evaluated through image correlation algorithm comparing images between before and after deformation [21]. Initially, unique correlation areas are defined as subsets, typically squared group of 10–25 pixels, and across the entire imaging area with overlapping of 2~3 pixels between adjoined subsets. The center of each subset is a measurement point that can be thought of as a virtual extensometer.

In this study, the physical features of objects' surface are substituted by virtual pattern generated by commercial DLP projectors. Thus, projected patterns are stationary in the image whether the objects are deformed or not. This means the virtually projected pattern cannot recognize relative 2D displacement, yet it still recognizes 3D shape profiles of each image among sequential images. By comparing 3D shape of objects obtained at each loading condition, the absolute 3D deformation can be effectively determined before and after loading.

In accordance with conventional 3D DIC, stereo cameras are calibrated determining position and angles together with optical parameters. Figure 2 shows the setup and process of determining the 3D shape profile for an object with 3D surface. This surface can be approximated by having many finite planes as parts of planes indicated virtual planes shown in Fig. 2b, which is a subset mentioned above. The subset positions with the image intensity values obtained from camera 1 that can be projected onto the corresponding virtual plane. The entire surface is approximated by consisting of many virtual planes illustrated by a red dash line in Fig. 2a. In order to profile a 3D shape of an object, positions of each virtual plane are located and correlated in the left and right camera coordinates.

As shown in Fig. 2b, the virtual plane can be coordinated by two direction angles (θ, $\varnothing$) to the normal vector of the plane and the variable distance Z_{position} denoting the location of the intersection of the plane and the optic axis for camera 1 (0, 0, Z_{position}). Thus, the virtual plane can be represented by the equation of plane as follows:

$$Z_{\text{position}} \cdot k = Z_{\text{camera 1}} \cdot k + X_{\text{camera 1}} \cos\theta + Y_{\text{camera 1}} cos\varnothing \quad (1)$$

where ($X_{\text{camera 1}}$, $Y_{\text{camera 1}}$, $Z_{\text{camera 1}}$) as a point on the plane, and $k = \sqrt{1-(\cos^2\theta + \cos^2\varnothing)}$.

Since setup for 3D DIC with projected pattern is basically followed by conventional 3D DIC calibration process, a virtual plane position is transformed from camera coordinates into image coordinates and finally located to CCD sensor

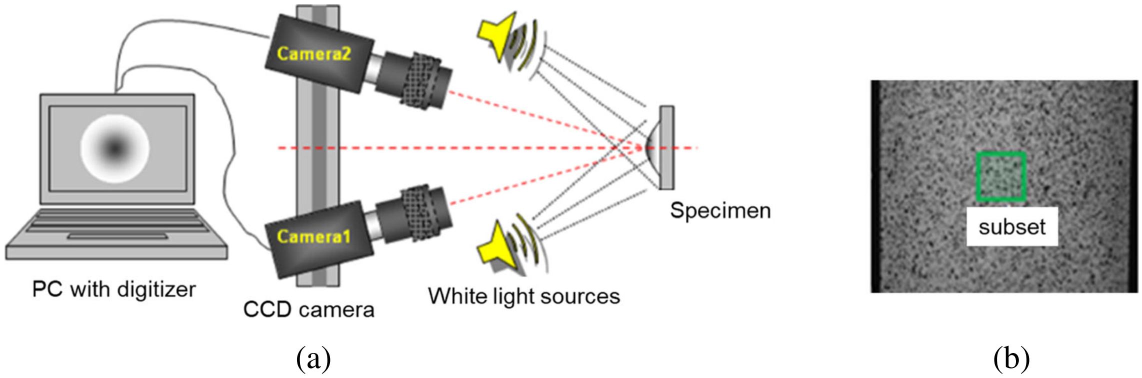

Fig. 1 **a** Schematic of 3-D DIC system; **b** specimen surface with speckle pattern, subset

coordinates. A physical relationship between the camera coordinate and sensor coordinate is to consider focal length f of used optical system and written as follows:

$$X_{camera}/X_{sensor} = Y_{camera}/Y_{sensor} = Z_{camera}/f \tag{2}$$

By combining Eqs. (1) and (2), $X_{camera\ 1}$, $Y_{camera\ 1}$, $Z_{camera\ 1}$ can be finalized in terms of $X_{sensor\ 1}$, $Y_{sensor\ 1}$, f_1, and written as Eq. (3).

$$X_{camera\ 1} = \frac{X_{sensor\ 1} Z_{position} k}{f_1 k + X_{sensor\ 1} \cos\theta + Y_{sensor\ 1} \cos\varnothing}, \quad Y_{camera\ 1} = \frac{Y_{sensor\ 1} Z_{position} k}{f_1 k + X_{sensor\ 1} \cos\theta + Y_{sensor\ 1} \cos\varnothing}, \quad Z_{camera\ 1} = \frac{f_1 Z_{position} k}{f_1 k + X_{sensor\ 1} \cos\theta + Y_{sensor\ 1} \cos\varnothing} \tag{3}$$

$X_{sensor\ 1}$ and $Y_{sensor\ 1}$ are determined representing location of subset in the CCD camera sensor. By conjugating each camera's result in the shared-wide coordinate system, the optimal position of the subset can be obtained.

Figure 3 describes the actual procedure to measure the 3D shape profile. The intensity values at the points on the selected subset from I_1 is compared with the intensity values at the projected points on I_2, both images taken at the same moment, via a virtual plane of (θ, $\varnothing$, and $Z_{position}$). For this, θ, $\varnothing$, and $Z_{position}$ are varied until I_1 and I_2 are matched through iterative correlation algorithm [22, 23], yielding 3D position and orientation of the matching virtual plane. Then, 3D positions on the surfaces are determined for the subset points. The 3D profiling can be completed by performing the same process for other subsets. Then, adjoining subsets are subsequently estimated for the position and orientation for full-field profile data. In the 3D DIC with projected pattern, these subsets are not supposed to be behaving as specimen deforms in x- and y-direction, which mean there is no image correlation achieved in 2D displacement. However, steady in-plane coordinate information does not affect the correlation of out-of-plane displacement.

Therefore, the feasibility of utilizing 3D DIC with virtual pattern can be confirmed for absolute 3D deformation measurement using schematic of 3D DIC shape profiling. 3D DIC without physical features of surface is very advantageous considering assessment of product warpage deformation during continuous

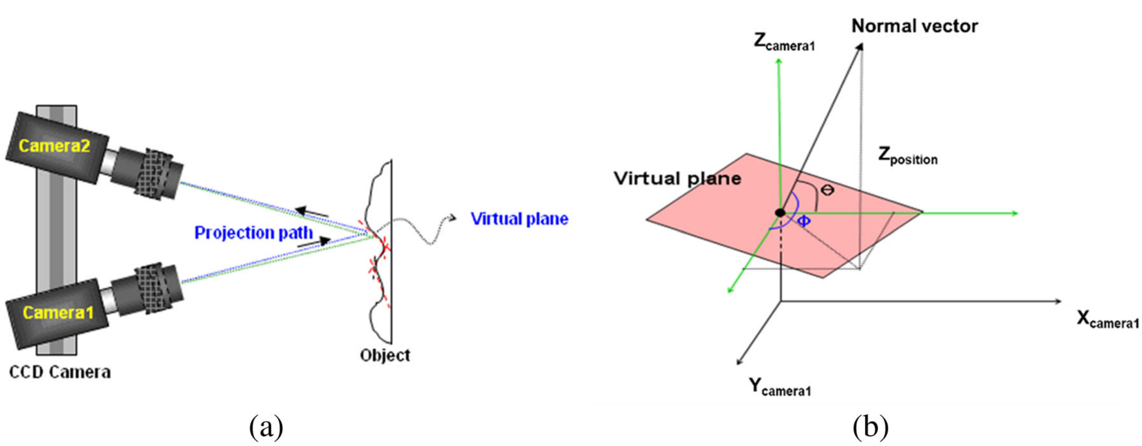

Fig. 2 **a** Schematic of the projection path to determine the orientation and 3-D position for subsets; **b** a plane generation with respect to camera coordinate

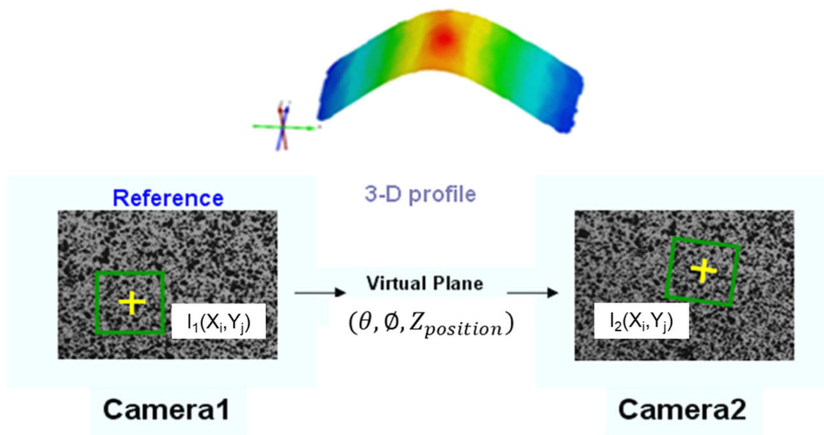

Fig. 3 Schematic of DIC procedure for the 3D shape profiling

manufacturing process or 3D deformation of very thin and fragile objects. In fact, in this study, a novel pattern-free 3D DIC measurement system was devised using DLP projector together with collimate lens system to measure smaller scale of object. This paper present successful warpage measurement of small-sized electronics package at elevated temperatures.

3 Virtual patterning using DLP projector

3.1 Experimental setup

DIC process requires recognizable intensity differences and high enough intensity values from the image, which can be achieved with a pattern consisting two very different colors. Previous researchers investigated and found that higher intensity of images by gray contrast effect generates more accurate DIC results [24, 25]. For an optimal use of DIC, the specimen has to be covered with speckle patterns. Usually, a random pattern with black dots on a white background provides excellent contrast levels in intensities. In this study, randomly distributed speckle patterns are easily generated by using an imaging software and projected onto the measured specimen shown in Fig. 4. Moreover, the projected pattern can be easily magnified by zoom lens of the DLP projector (Fig. 4a). Figure 4b shows opened image of subset (15 × 13 pixels) with gray-scale values for individual pixel. There are three benefits of 3D DIC with projected patterning method. The first is to control speckle size and distribution, which affects the intensity values of subsets. The second is that size of projected pattern can be adjusted in accordance with FOV size by using any drawing software in the PC. The third is that does not involve any physical sample preparation.

The entire configuration of experimental setup is shown in Fig. 5. Two high-resolution Marlin CCD cameras (1628 × 1236 pixels) with 75 mm Pentax lenses take a place in a stereo-vision system facing the specimen at two different locations. On the specimen, a high-contrast speckle pattern is projected by a commercial DLP projector. A typical DLP projector consists of projection lens system as a zoom lens, which enlarges image size. This means that the pattern image projected is magnified too much to focus the optimal density

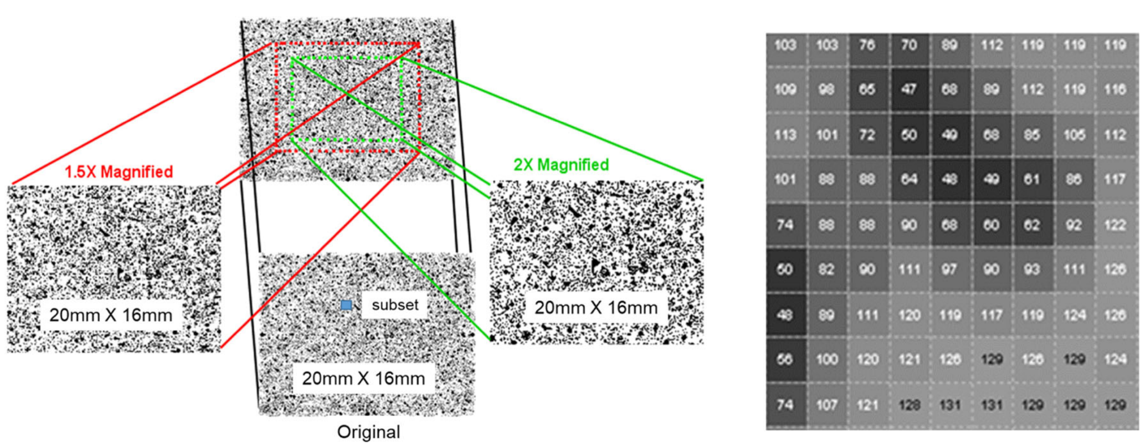

(a) (b)

Fig. 4 Arbitrary drawn speckle patterns using an imaging software. **a** Original pattern image is magnified by factor of 1.5 and 2: **b** opened image of subset with speckles bigger than 1 pixel of radius and pixel values

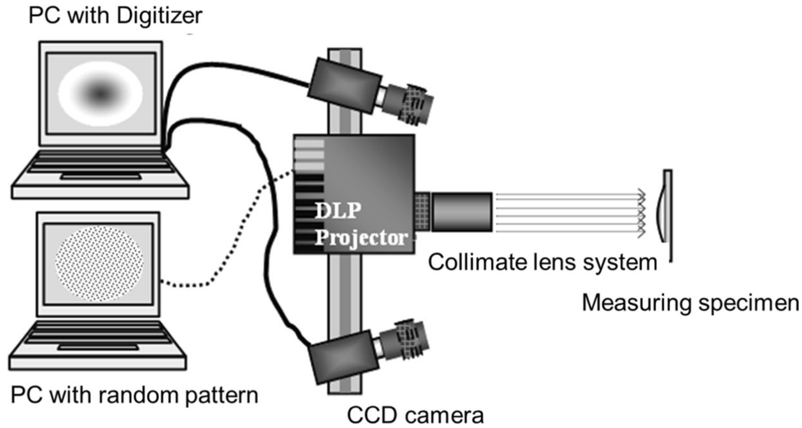

Fig. 5 Configuration of 3D DIC system with pattern projection system

of pattern on the surface of small objects. Thus, a collimate lens system was designed to adjust pattern image size appropriately for projecting in a small scale. As shown in Fig. 6, designed collimate lens system simply consists of two lenses combining a single gradient index lens and a molded aspheric glass lens. According to mechanism of optics, projected image size can be adjustable as projection lens's focal length changes, which are denoted as F and d in Fig. 6. As a result, this lens array system not only prevents the divergence of light caused by a projection lens system, but also provides long enough working distance. In this particular case, distance between object and lens system is approximately 170 mm with 15 mm × 15 mm pattern image size.

Both cameras are calibrated using conventional 3D DIC calibration process and FOV size was adjusted to be 15 mm × 15 mm in consideration of a small electronics package size.

4 Validation of 3D shape profile measurement

As mentioned earlier, there is no need for treatment of sample surface. It is expected that the projected surface profile obtained by 3D DIC should be resulting as close as its real profile. For the validation, as shown in Fig. 7, a plastic package with convex surface is selected for profiling, and a pattern image of randomly distributed speckles is projected on the region of interest (FOV) through a DLP projector with collimate lens system.

In order to assess the feasibility of projecting pattern for DIC, the surface profile is measured by both DIC and Wyko surface profilometer (Veeco®), which is well-known for nanometers of measurement sensitivity, and then the results obtained by two methods have been compared. It should be noticed that Wyko profilometer is limited to measure small FOV size, which means it took a long time to measure this specimen, while 3D DIC took a second. As shown in Fig. 7, although it is 35 mm × 35 mm size of package, only 15 mm × 15 mm size of middle area is profiled at room temperature.

Figure 8 shows its topography obtained using DIC and Wyko profilometer. Both results show an excellent agreement in contour plots. For a quantitative observation, a diagonal line indicated as a white dash line in Fig. 8a, has been drawn after eliminating rigid body motion so that the surface profiles along this line can be plotted as shown in Fig. 8b. The measured surface was originally convex shape and its 3D shape profile was measured 157 μm from Wyko and 151 μm from 3D DIC respectively. It is about 96% close to each other, and this proves the high accuracy of developed 3D DIC with virtual patterning method.

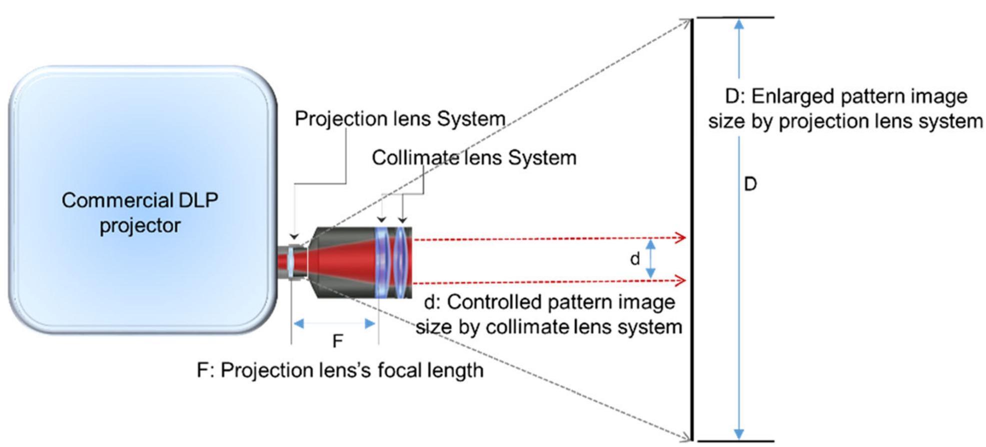

Fig. 6 Collimate lens system to focus reduced FOV size

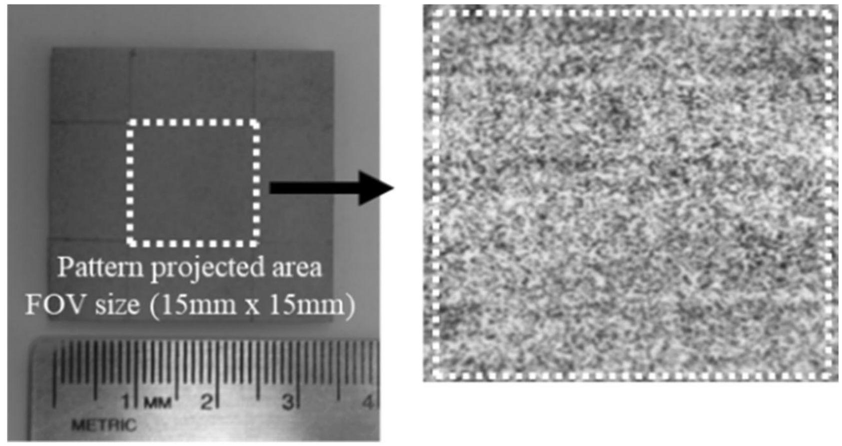

Fig. 7 Convex shape of a plastic package and speckle pattern projected onto surface with white dashed area for 3D DIC measurement

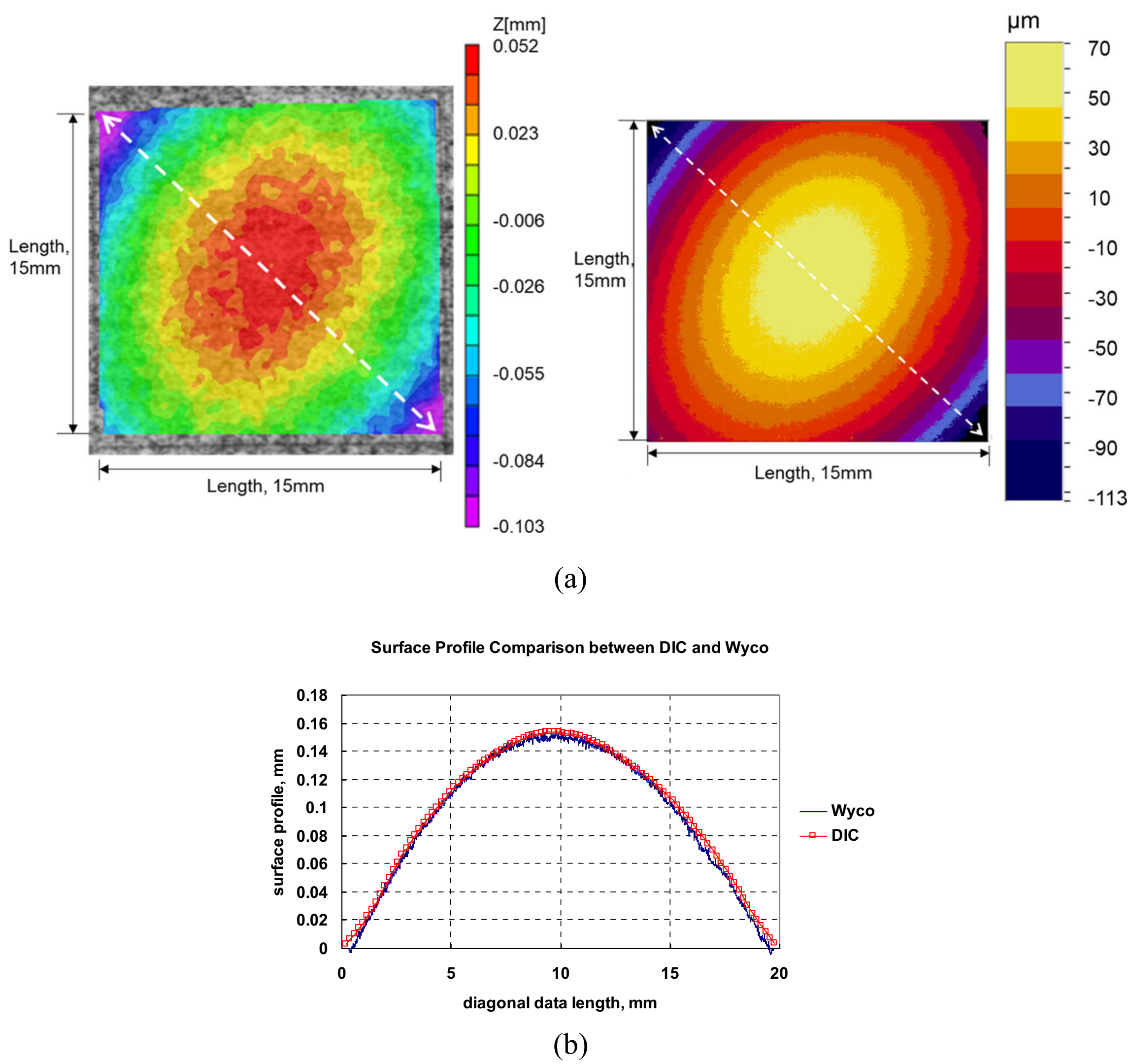

Fig. 8 **a** Surface profile by DIC, left, and Wyko Profilometer, right, and **b** comparison of surface profile between DIC and Wyko Profilometer

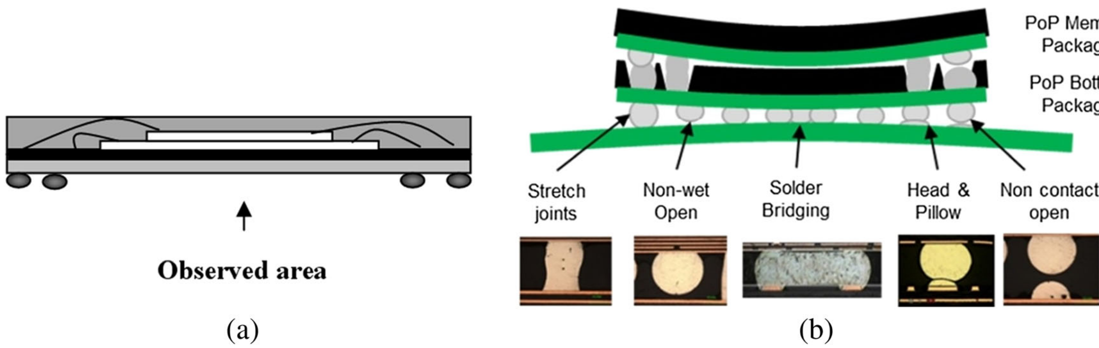

Fig. 9 **a** Measured memory package of POP (top portion of PoP package); **b** typical defect mode of POP during manufacturing process due to warpage [21]

5 Warpage measurement of top portion of PoP package

In this study, a PBGA package (PoP memory package shown in Fig. 9a with 15 mm × 15 mm × 1 mm size is considered for warpage measurement. This particular electronics package consists of various materials are shown in Fig. 9a, such as chip, substrate (organic printed circuit board), and plastic encapsulation. The structure shows that two chips are bonded using die attachment and wire bonded to substrate, then molded by plastic encapsulation. Due to the nature of composite, the package easily experiences out of plane deformation during surface mounting manufacturing process, which is carried out at elevated temperatures. Materials used to this package have different coefficient of thermal expansion resulting in warpage behavior and sequentially causing various defects throughout assembly process as shown in Fig. 9b. Therefore, the warpage measurement of electronic package is major concern to understand thermomechanical reliability.

The experimental setup is shown in Fig. 10. The PoP memory package is placed inside of environmental chamber, with its FOV focused by a pair of Marlin CCD camera. There is a DLP projector with collimate lens system projecting speckle patterns onto the bare bottom surface of the PoP package through the window of environmental chamber. Images are taken while the specimen is exposed to convectional heating from a room temperature of 150 °C, at 25 °C, 50 °C, 100 °C, 150 °C, and after cooling back to 25 °C. Pairs of images taken simultaneously before, during and after heating, can be seen using a software and subjected to image correlation. For the result, different surface profiles are obtained at each elevated temperature.

The contour plot of surface profile at room temperature is shown in Fig. 11a. As shown, the bottom surface of PoP memory package is shaped diagonally symmetric. Figure 11b shows the measured surface profiles after rigid body movement correction at elevated temperatures along the diagonal 0 and diagonal 1 respectively, and they are considered as absolute warpages. The package warps in positive direction in z-axis as temperature increases. While the package is exposed to various temperatures from room temperature to 150 °C, the maximum warpage values along diagonal 0 and 1 are approximately 12 and 15 μm respectively. In addition,

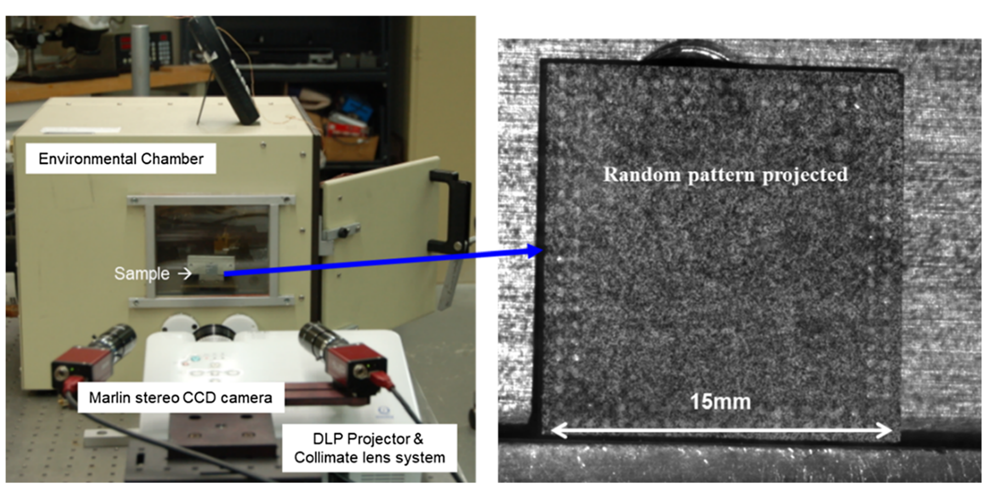

Fig. 10 Test setup for warpage measurement

Fig. 11 Warpage behaviors of PBGA package measured by 3D DIC with virtual patterning method. **a** Surface profile at room temperature; **b** surface profiles of diagonal 0 and 1 at various elevated temperature from left to right respectively; **c** 3D contour plots of the PoP memory package at various temperatures

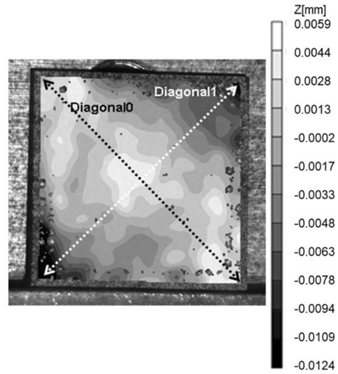

(a) Surface profile at room temperature

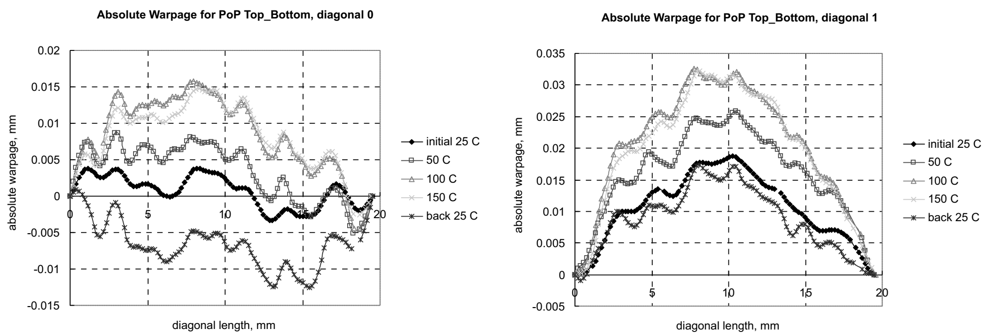

(b) Surface profiles of diagonal 0 and 1 at various elevated temperature from left to right respectively

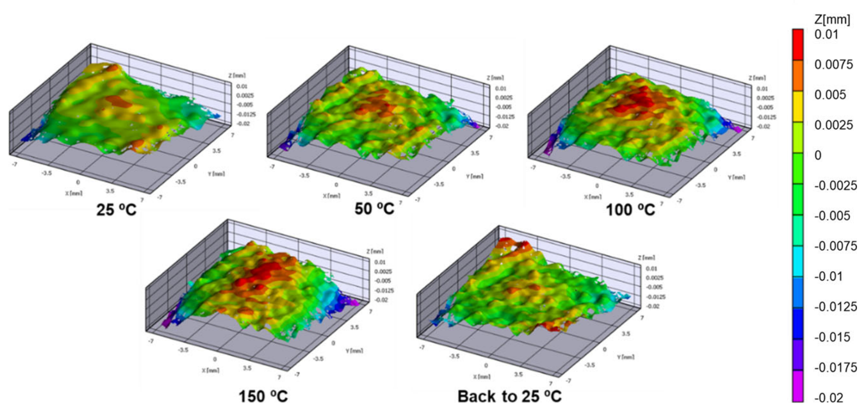

(c) 3D Contour plots of the PoP memory package at various temperatures

since the warpage difference between 100 and 150 °C is relatively small, it is expected that the curing temperature of die attachment was in between 100 and 150 °C. In addition, when it has cooled down to room temperature, the shape has not been completely recovered in the direction of diagonal 0 possibly due to moisture effect inside the package. Each surface profile is plotted in 3D contour map shown in Fig. 11c, so that the changes of shape can be seen more visually.

From the in situ 3D DIC with projected pattering method, actual warpage behavior of POP memory package is understood. First of all, the amount of solder paste needs to be optimized for the surface mount process between top and bottom portion of POP packages and PCB during manufacturing. Second of all, repeatable warpage behavior of the package would cause thermos-mechanical fatigue at the solder joints. Therefore, design for reliability of the POP package has to be considered.

6 Summary

The feasibility of the pattern projection method for 3D DIC measurement is investigated. Virtual pattern generated by DLP projection yield good results in 3D DIC, and this has been proved by the warpage measurement of electronic package 15 mm × 15 mm size. In addition, since this method does not involve any surface treatment of a specimen, it represents an actual profile of specimen, which was validated by optical profiler. It is highly advantageous that no sample preparation is required. Although the pattern projection method cannot be applied to in-plane displacement (2D) measurement or tracking relative 3D deformations, it can be applied to shape profiling or warpage measurement as shown above. Moreover, it has been discovered that the light divergence of DLP projector can be prevented by using lens system with combination of different lenses. By doing so, the projected pattern is well focused on the specimen's surface (small area) at a distance. Moreover, the pattern projection method offers the flexibility of controlling speckle sizes without losing the stochastic randomness of pattern, which is the pattern requirement for DIC measurement, even when the FOV size is smaller than 15 mm. Non-contamination warpage measurement enables the industry to examine their products' behavior subjected to various loading and continuously monitor qualities of assembly during manufacturing process.

References

1. Wakharkar V, Matayabas C, Lehman E (2005) Materials technologies for thermomechnical management of organic packages. Intel Technol J 09(04)
2. Chien IY, Zhang J, Rector L (2007) Low-warpage molding compound development for array packages. Global SMT & Packaging
3. Sharpe WN Jr (2008) Springer handbook of experimental solid mechanics. Springer Science + Business Media, LLC, New York
4. Yaakobovitz A, Krylov S, Hanein Y (2010) Nanoscale displacement measurement of electrostatically actuated micro-devices using optical microscopy and digital image correlation. Sensors Actuators A 162:1–7
5. Kang D-J, Chen F, Park J-H (2014) New measurement method of Poisson's ratio of thin films by applying digital image correlation technique. Int J Precis Eng Manuf 15(5):883–888
6. Min H-G, Kang D-J, Kim KJ, Park J-H (2017) New non-contact measurement method of deformation at tensile test of thin film via digital image correlation technique. Int J Precis Eng Manuf 18(11): 1509–1517
7. Chen F, Kang D-J, Park J-H (2013) New measurement method of Poisson's ratio of PVA hydrogels using an optical flow analysis for a digital imaging system. Meas Sci Technol 24:055602
8. Roland T, Arscott S, Sabatier L, Buchaillot L, Charkaluk E (2011) Digital image correlation of metal nanofilms on SU-8 for flexible electronics and MEMS. J Micromech Microeng 21:125005
9. Baqersad J, Poozesh P, Niezrecki C, Avitabile P (2017) Photogrammetry and optical methods in structural dynamics-a review. Mech Syst Signal Process 86 (17–34
10. Cheong K, Omer K, Butcher C, George R, Dykeman J (2017) Evaluation of the VDA 238-100 tight radius bending test using digital image correlation strain measurement. J Phys Conf Ser 896:012075
11. Cofaru C, Philips W, Van Paegegem W (2012) A three-frame digital image correlation (DIC) method for the measurement of small displacements and strains. Meas Sci Technol 23:105406
12. Li G, Gengxiang X, Sun G, Le Q (2014) Identification of mechanical properties of the weld line by combining 3D digital image correlation with inverse modeling procedure. Int J Adv Manuf Technol 74:893–905
13. Liu J, Liu X, Yang L, Liang H (2013) Determination of flow stress of thin-walled tube based on digital speckle correlation method for hydroforming applications. Int J Adv Manuf Technol 69:439–450
14. Kwak JB (2014) Strain behaviors of solder bump with underfill for flip chip package under thermal loading condition. J Mech Sci Technol 28(12):4899–4906
15. Wang H, Xie H, Dai X, Zhu J (2013) Fabrication of a DIC sensor for in-plane deformation measurement. Meas Sci Technol 24: 065402
16. Chen Z, Quan C, Zhu F, He X (2015) A method to transfer speckle patterns for digital image correlation. Meas Sci Technol 26:095201
17. Fan SH, Chan YC (2002) Effect of misalignment on electrical characteristics of ACF joints for flip chip on flex applications. Microelectron Rel 42(7):1081–1090
18. Kwak JB, Park S (2015) Integrated hygro-swelling and thermomechanical behavior of mold compound for MEMS package during reflow after moisture preconditioning. Microelectron Int 32(1):8–17
19. Srikanth N (2006) Warpage analysis of epoxy molded packages using viscoelastic based model. J Mater Sci 41(12):3773–3780
20. Johnson SC (2007) Package-on-package technology evolves. Semiconductor International
21. Loh WK, Haley F (2016) Package-on-package warpage characteristics and requirements. SMT Magazine:68–69
22. Sutton MA, McNeill SR, Helm JD, Chao YJ (2000) Advances in two-dimensional and three-dimensional computer vision. Photomechanics Topics Appl Phys 77:323–372
23. Sutton MA, Yan J, Deng X, Cheng C-S, Zavattieri P (2007) Three-dimensional digital image correlation to quantify deformation and crack-opening displacement in ductile aluminum under mixed-mode I/III loading. Opt Eng 46(5)
24. Zhu H, Liu X, Chen L, Ma Q, Ma S (2018) Influence of imaging configurations on the accuracy of digital image correlation measurement. Meas Sci Technol 29:035205
25. Ferrer B, Mas D (2018) Parametric evaluation of errors using isolated dots for movement measurement by image cross-correlation. Sensors 18:525